

V. F. Nesterenko,<sup>a)</sup> M. A. Meyers, H. C. Chen, and J. C. LaSalvia  
 Institute for Mechanics and Materials, Department of Applied Mechanics and Engineering Sciences,  
 University of California, San Diego, California 92093

(Received 15 July 1994; accepted for publication 12 October 1994)

It is demonstrated that controlled high-strain-rate plastic deformation of heterogeneous reactive porous materials (Nb+Si, Mo+Si+MoSi<sub>2</sub>) produces shear localization. Within the shear bands, having thicknesses 5–20 μm, the overall strains (γ≤100) and strain rates (γ̇≤10<sup>7</sup> s<sup>-1</sup>) result in changes in particle morphology, melting, and regions of partial reaction. The shear band thickness is smaller than the initial characteristic particle size of the porous mixture (≤44 μm). This ensures quenching of the deformed material structure in the same time scale as the deformation time (10<sup>-5</sup> s). In the shear localization region, two types of patterning are observed: (a) a characteristic shear fracture which subdivides the Nb particles into thin parallel layers and (b) the formation of vortices. © 1994 American Institute of Physics.

It is well known that phase transitions and chemical reactions can be produced by shock compression, and it has been suggested that shear deformation plays an important role.<sup>1–3</sup>

The thick-walled cylinder method,<sup>4,5</sup> which was developed for the investigation of deformation and shear localization processes in solid materials (metals, polymers) at high strain rates was modified for this investigation. Figure 1 shows one of the configurations used. A porous Nb–Si mixture (68%–32% by weight), with particle sizes smaller than 44 μm (–325 mesh), initial density 2 g/cm<sup>3</sup> was placed in a tubular cavity between a central copper rod (diameter 16.2 mm) and an outer copper tube (i.d. 20 mm and o.d. 30.8 mm). An explosive [explosive 1, Fig. 1(a)] with low detonation velocity (2.5 km/s) was used to densify this mixture to a density of 3.2 g/cm<sup>3</sup>. Detonation was initiated on the top of the charge and propagated along cylinder axis. No shear localization was observed after this step because the overall plastic deformation is sufficiently small (final diameter of inner surface of driving copper cylinder is equal to 18.7 mm). A cylindrical hole with diameter 11 mm was drilled [Fig. 1(b)] along longitudinal axis of copper rod and this composite cylinder was collapsed by the detonation of a second cylindrical explosive charge [explosive 2, Fig. 1(b)] with detonation velocity of 4 km/s, density 1 g/cm<sup>3</sup>, and o.d. 60 mm.<sup>4,5</sup> This second explosive event produces significant plastic deformation in the densified porous layer which is highly localized in shear bands and not homogeneously distributed [Figs. 1(c) and 1(d)]. The average values of *r* and *r*<sub>1</sub> are equal 5.9 and 7.5 mm, respectively. A second configuration was used for the same powder with the same initial density of 2 g/cm<sup>3</sup>. It was placed in the tubular cavity with inner and outer diameters 16.4 and 21.7 mm [analogous to Fig. 1(b)]. A preexisting hole along the longitudinal axis of assembly, with a diameter of 11 mm, ensured high plastic deformation directly applied to the porous material. A few layers of amorphous ribbon (23 μm thick) were placed along the cylinder walls to initiate shear localization in powder, with lower density, at an early stage of collapse of inner hole.

The average values of *r* and *r*<sub>1</sub> after collapse were equal to 6.5 and 8.1 mm and plastic deformation was highly localized, as in Figs. 1(c) and 1(d), for first configuration. A third configuration, which was applied to the porous mixture MoSi<sub>2</sub>+Mo+Si in a steel container, was also used. It is described in detail elsewhere.<sup>6</sup> The overall radial and tangential strains (*e*<sub>rr</sub> and *e*<sub>φφ</sub>) of incompressible material, before the onset of localization, can be estimated knowing the initial and final radii ρ<sub>0</sub> and ρ at a general point:

$$e_{rr} = \frac{\rho_0}{\rho} - 1, \quad e_{\phi\phi} = \frac{\rho}{\rho_0} - 1. \quad (1)$$

The final radii ρ and *R* (or *R*<sub>1</sub>) and initial radius *R*<sub>0</sub> (or *R*<sub>10</sub>)

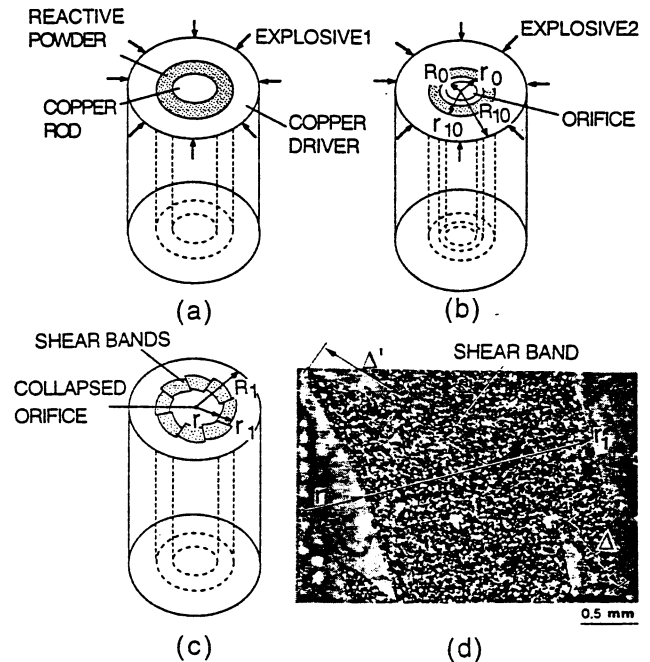


FIG. 1. Sequence of deformation events in thick-walled cylinder method: (a) initial geometry, (b) powder densified and drilling of central orifice, (c) final configuration, (d) general view of shear localization in porous Nb–Si mixture (configuration 1).

<sup>a)</sup>On leave from Lavrentyev Institute of Hydrodynamics, Russian Academy of Sciences, Novosibirsk, 630090, Russia.

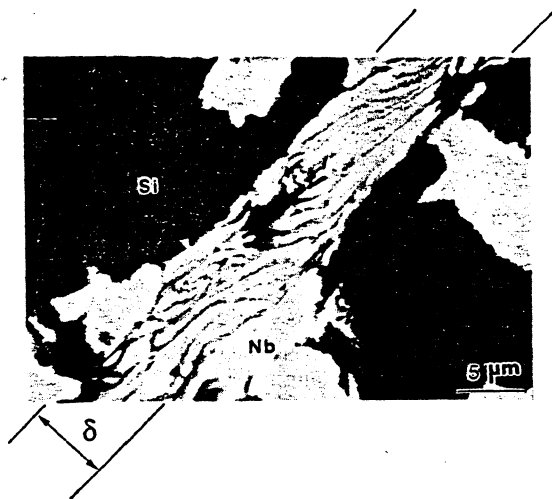


FIG. 2. Fracture patterning of Nb particle inside shear band (configuration 1); Nb is white, Si is dark, boundaries of shear band are shown by lines on the back.

[Figs. 1(b)–1(d)] are experimentally measured and the value of  $\rho_0$ , which corresponds to selected value of  $\rho$ , can be calculated using Eq. (2):

$$\rho_0^2 = \rho^2 + R_0^2 - R^2 = \rho^2 + R_{10}^2 - R_1^2. \quad (2)$$

The overall strain in copper at the boundary with the porous layer outside the shear localization region can be estimated using Eq. (1). For configuration 1, after first explosive event: at  $\rho=r_{10}$ ,  $e_{rr} \approx 0.07$  and  $e_{\varphi\varphi} \approx -0.07$ . After second explosive event: at  $\rho=r_1$ ,  $e_{rr} \approx 0.25$ ,  $e_{\varphi\varphi} \approx -0.2$ ; at  $\rho=r$ ,  $e_{rr} \approx 0.37$ , and  $e_{\varphi\varphi} \approx -0.27$ . For second configuration: at  $\rho=r_1$ ,  $e_{rr} \approx 0.34$  and  $e_{\varphi\varphi} \approx -0.25$ ; at  $\rho=r$ ,  $e_{rr} \approx 0.26$ ,  $e_{\varphi\varphi} \approx -0.21$ . Note that deformation in copper under these conditions is homogeneous.<sup>4,5</sup>

Figure 1(c) shows, in schematic fashion, the nonhomogeneous nature of the plastic deformation of the porous mixture; this is very clearly seen in Fig. 1(d), in which one shear localization region is depicted. The shear localization regions make an angle of  $45^\circ$  with the radius (direction of maximum shear stress). The overall shear strain inside the shear zone is the ratio of the amplitude of shear  $\Delta$  [Fig. 1(d)] and thickness of shear band  $\delta$  ( $\gamma \sim \Delta/\delta$ ). This scheme yields “uniform” shear localization with approximately equal displacements ( $\Delta, \Delta'$ ) at inner and outer surfaces of the porous mixture [Fig. 1(d)], as a result of relatively close overall strains  $e_{rr}$ ,  $e_{\varphi\varphi}$  at  $r$  and  $r_1$ . The shear displacements  $\Delta \sim 100$ – $600 \mu\text{m}$  and shear band thicknesses  $\delta \sim 5$ – $10 \mu\text{m}$  for initial density of  $3.2 \text{ g/cm}^3$  and  $10$ – $20 \mu\text{m}$  for density of  $2 \text{ g/cm}^3$ , Figs. 2–4) enable the evaluation of shear strain in the range  $10$ – $100$ .

The kinetics of uniform overall deformation can be determined from the measurement of the inner surface velocity of the wall,  $V_i$ .<sup>5</sup> The radial and tangential strain rates are

$$\begin{aligned} \dot{e}_{rr} &= - \frac{(\rho^2 + R_0^2)^{1/2}}{[\rho^2 + R^2(t)]^{3/2}} V_i(t)R(t), \\ \dot{e}_{\varphi\varphi} &= \frac{V_i(t)R(t)}{(\rho^2 + R_0^2)^{1/2}[\rho^2 + R^2(t)]^{1/2}}, \end{aligned} \quad (3)$$

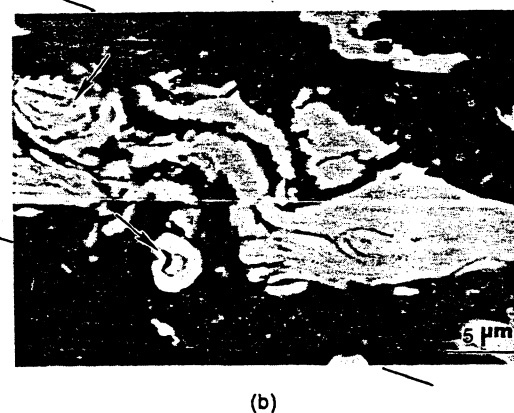
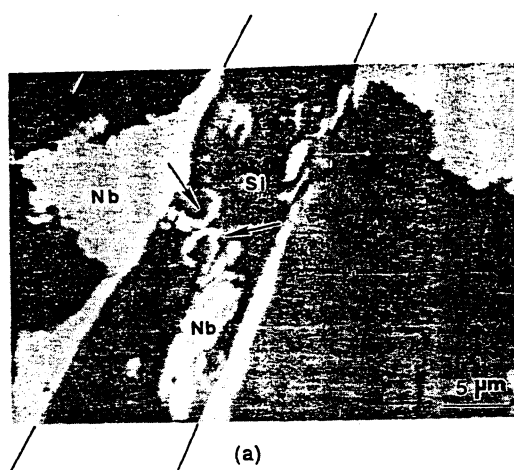


FIG. 3. Vortex formation (see arrows) inside shear band; (a) configuration 1, (b) configuration 2.

where  $V_i(t)$  and  $R(t)$  are the time-dependent velocities of inner surface and radius of hole, respectively. It is assumed that the hole is fully closed in the collapse process (i.e.,  $R=0$ ) and that the collapse process is not significantly altered by the insertion of the porous material layer; therefore, measurements for copper cylinder were used. Strain rates, calculated from Eq. (3), on the basis of the measurement of  $V_i(t)$ , provide values in the range  $(1.5$ – $4) \cdot 10^4 \text{ s}^{-1}$  for configurations 1 and 2. The average shear strain rate inside the shear zone can be determined from measurement of time of the deformation process (time of pore collapse  $\tau \approx 8 \mu\text{s}$ ) and shear strain  $\gamma$ :  $\dot{\gamma} \approx \gamma/\tau$ . Shear strain rates are  $10^6$ – $10^7 \text{ s}^{-1}$  for shear bands with different values of  $\Delta$ ,  $\delta$ . From the measurements of inner surface velocity,<sup>5</sup> it is possible to calculate the inertial compression stress in the porous layer; it is found to be less than  $0.1 \text{ GPa}$ .

The following qualitative features of high-rate shear localization in porous two-component mixtures were established:

(1) The shear localization results in partial melting of one component (Si), as in shock wave loading.<sup>3</sup> The small thickness of the shear band is responsible for quenching of the material and retention of reaction products formed during deformation process. Taking the thermoconductivity coeffi-

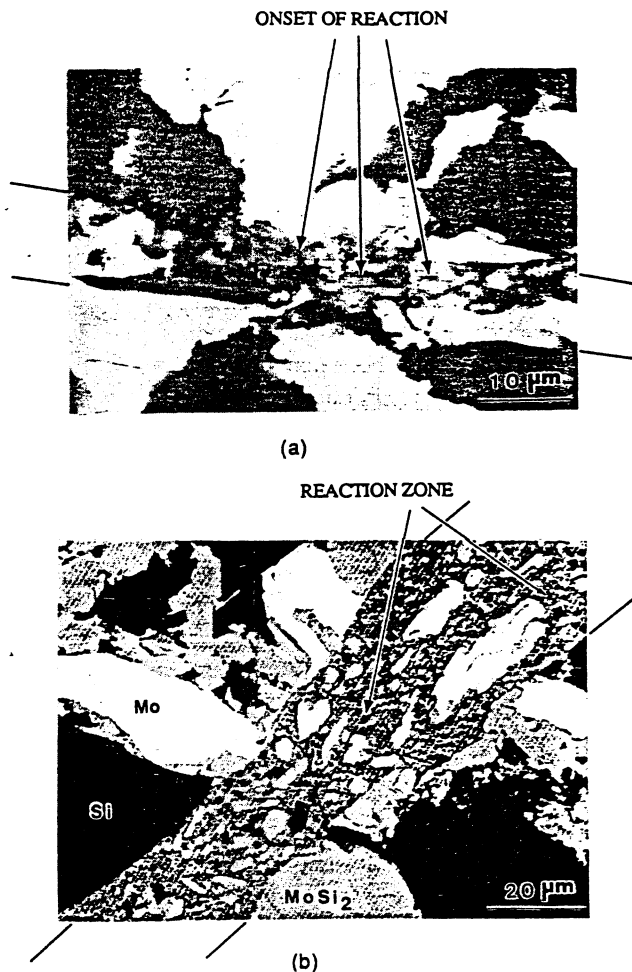


FIG. 4. Partially reacted material (see arrows) inside shear band; (a) configuration 2, (b) configuration 3.

cient for surrounding material as  $\sim 0.1 \text{ cm}^2/\text{s}$ , and  $\delta \approx 10 \text{ }\mu\text{m}$ , quenching time  $\sim 10^{-5} \text{ s}$  and quenching rate  $\sim 10^8 \text{ K/s}$  are obtained.

(2) The multiple fracturing of Nb particles due to shear localization, at the mesolevel, leads to a decrease of initial particle size from 44 to 1–2  $\mu\text{m}$ , and produces a unique fracture patterning inside the shear zone (Fig. 2). This behavior is qualitatively different from the one of Nb particles in shock-wave compression with amplitude up to 30 GPa.<sup>3</sup>

(3) Material flow inside the shear band is unstable and results in vortex formation (Fig. 3) which can drastically enhance the heat and mass transfer. Arrows show the regions where the thin layers, resulting from the shear fracture of the Nb particles (white), mark the rotations in the flow pattern. The minimum rotational frequency  $\omega$  inside the vortex can be evaluated because the time of the process ( $\tau \approx 10^{-5} \text{ s}$ ) and vortex diameter ( $d \approx \delta/4 \approx 3 \text{ }\mu\text{m}$ ) [Fig. 3(a)] are known. From these parameters, the corresponding rotational frequency is  $\omega \sim 7 \times 10^5 \text{ s}^{-1}$ . Patterning inside the shear zone due to either thermal or nonlocal effects (described by high order gradient models) was recently predicted by Molinari and Leroy.<sup>7,8</sup> It is possible that vortex formation (Fig. 3) can be explained by a nonlocal mechanism; gradients in flow stresses due to the

heterogeneity of mixture are a possible cause.<sup>8</sup> An alternative explanation can be based on the hydrodynamic instability of flow inside shear zone. The Reynolds number  $Re$  for material flow inside the shear band can be evaluated assuming that Si is completely molten and its viscosity  $\nu$  has a value typical for liquids,  $0.01 \text{ cm}^2/\text{s}$ . The overall average velocity  $V$  of flow can be calculated as  $V \approx \Delta/\tau$ . For  $\Delta \approx 600 \text{ }\mu\text{m}$ ,  $\tau \approx 8 \text{ }\mu\text{s}$ ,  $V$  is approximately equal to 75 m/s. The corresponding Reynolds number for the flow inside shear band if  $\delta \approx 10 \text{ }\mu\text{m}$  is  $Re = V \cdot \delta/\nu \approx 750$ . The hydrodynamic flow instability inside shear band demands a critical Reynolds number from 3100 to 4000.<sup>9</sup> This can hardly be developed under these conditions, considering that the assumed viscosity of Si is the lowest limit. Nevertheless, this mechanism cannot be ignored, because material inside shear band is not homogeneous as the shear thickness is not uniform (Figs. 3 and 4).

(4) The intermetallic reaction between molten Si and fractured Nb proceeded in some regions [Fig. 4(a)]: there are only some places inside cracks in Nb and rounded small particles inside Si with diameters less than 8  $\mu\text{m}$  that can be considered reaction spots; they were identified by energy dispersive x-ray analysis. The evidence of reaction is clear in Fig. 4(b) corresponding to the initial mixture  $\text{MoSi}_2 + \text{Mo} + \text{Si}$ . The white (Mo), black (Si), and gray ( $\text{MoSi}_2$ ) regions outside of the shear zone are replaced by gray material inside it, showing that reaction between Mo and Si took place. Reactions were not observed outside shear zones. These results are in accord with a recent report<sup>10</sup> of shock induced formation of  $\text{MgAl}_2\text{O}_4$  spinel upon shock loading of single crystals (corundum- $\text{Al}_2\text{O}_3$  and periclase- $\text{MgO}$ ) at the contact interface in oblique impact experiments (shock pressures 26–36 GPa).

(5) The shear-band thickness has a tendency to increase with the decrease of initial density of powder [Figs. 2 and 3(a) relate to initial density of  $3.2 \text{ g/cm}^3$  and Figs. 3(b) and 4(a) to  $2 \text{ g/cm}^3$ ] and does not coincide with the initial particle size in the mixture.

The authors would like to thank A. Molinari for valuable discussions, R. J. Skalak for support, G. Velasco for help in manuscript preparation, and M. S. Hsu for metallography. This research is supported by the U. S. Army Research Office, Contract No. DAAH 04-94-G-031, U.S. Office of Naval Research, Contract No. N00014-94-1-1040, National Science Foundation, Grant No. MSS 90-21671, and the Institute for Mechanics and Materials, UCSD.

<sup>1</sup>R. A. Graham, *Solids Under High Pressure Shock Compression: Mechanics, Physics and Chemistry* (Springer, New York, 1993).

<sup>2</sup>A. N. Dremin and O. N. Breusov, *Russ. Chem. Rev.* **37**, 392 (1967).

<sup>3</sup>M. A. Meyers, L.-H. Yu, and K. S. Vecchio, *Acta Metall. Mater.* **42**, 715 (1994).

<sup>4</sup>V. F. Nesterenko, A. N. Lazaridi, and S. A. Pershin. *Fiz. Goreniya Vzryva* **25**, 154 (1989) (in Russian).

<sup>5</sup>V. F. Nesterenko, M. P. Bondar, and I. V. Ershov, in *High-Pressure Science and Technology—1993*, edited by S. C. Schmidt *et al.* (AIP, New York, 1994), p. 1172.

<sup>6</sup>M. A. Meyers and S. L. Wang, *Acta Metall.* **36**, 925 (1988).

<sup>7</sup>A. Molinari and Y. M. Leroy, *C. R. Acad. Sci. Paris* **313**, 7 (1991).

<sup>8</sup>Y. M. Leroy and A. Molinari, *J. Mech. Phys. Solids* **41**, 631 (1993).

<sup>9</sup>H. L. Dryden, F. D. Murnaghan, and H. Bateman, *Hydrodynamics* (Dover, New York, 1956).

<sup>10</sup>D. K. Potter and T. J. Ahrens, *Geophys. Res. Lett.* **21**, 721 (1994).